Available online at www.sciencedirect.com

ScienceDirect

Ceramics International 39 (2013) 9391–9396

CERAMICS INTERNATIONAL

www.elsevier.com/locate/ceramint

Mechanical properties and microstructure of fast fired tiles made with blends of kaolin and olivine powders

E. Furlani*, S. Maschio

Università di Udine-Department of Chemistry, Physics and Environment, Via del Cotonificio 108, 33100 Udine, Italy

Received 27 February 2013; received in revised form 29 April 2013; accepted 29 April 2013
Available online 23 May 2013

Abstract

The paper reports on some experimental results obtained from the production of ceramic tiles containing olivine and kaolin powders mixed in different proportions. Blending of components was done by attrition milling. Pressed powders were fast fired (55 min cold to cold) in air up to 1250 °C. Fired products were characterized by shrinkage, water absorption, density, strength, hardness, toughness, crystal phases and microstructure. It has been demonstrated that all the samples prepared have properties in line with the industrial production of some ceramic materials, but those containing 60 wt% of olivine and 40 wt% of kaolin displayed the best overall behaviour and therefore the blend is a possible candidate of an eventual industrial production of tiles.

Keywords: C. Mechanical properties; Tiles; Rapid sintering; Olivine

1. Introduction

In a previous paper [1] we described blending, sintering behaviour and crystal phases evolution of several ceramics containing mixtures of waste olivine powders (O) and a high grade kaolin (K). It was demonstrated that all materials complete the first part of the sintering process (high open porosity) below 1100 °C and enter into the final sintering stage between 1150 and 1200 °C as a function of their compositions; during this stage their water absorption lowers below 5%. All mixtures progressively soften when fired at temperatures higher than 1300 °C and samples loose their shape due to the presence of the liquid phase. On the progress of that research, here we report further experimental results obtained, when the previously studied O/K blends are used to prepare tiles, fired in rapid sintering cycle at 1250 °C, as pre-industrial type testing experiments in order to investigate if materials fired at their optimal temperature could represent an option for the possible recycling of the waste olivine into the production of tiles.

The final products were then characterized by crystal phases, shrinkage, water absorption, density, bending strength, hardness, fracture toughness and microstructure.

The aim of the present paper is to demonstrate that, proper quantity of waste products (i.e. olivine) can be used, mixed with natural raw materials, in the production of tiles that satisfy most of the official standards.

2. Materials and methods

The O powders used in the present work result from a depulverization metallurgical process which makes olivine sands suitable for moulds preparation before the casting of high manganese steels. Their chemical and crystallographic characteristics are those of natural olivines, but powders particles have size below 20 μm. They were blended with 20, 40, 60 and 80 wt% of a high grade K. Symbols used for samples identification are respectively OK20, OK40, OK60 and OK80, the same as those of the previous research.

The chemical composition O and K, obtained by a Spectro Mass 2000 Induced Coupled Plasma (ICP) mass spectrometer, is reported in Table 1 which also displays lost on ignition (LOI) after a thermal treatment at 1000 °C for 2 h.

*Corresponding author. Tel.: +39 432558863/77; fax +39 432558803.
E-mail addresses: erika.furlani@uniud.it (E. Furlani), stef.maschio@uniud.it (S. Maschio).

0272-8842/$ - see front matter © 2013 Elsevier Ltd and Techna Group S.r.l. All rights reserved.
http://dx.doi.org/10.1016/j.ceramint.2013.04.113

Table 1
Composition (wt%) and LOI (%) of Kaolin (K) and Olivine (O) used as starting materials in the present study.

Component	Kaolin	Olivine
SiO_2	47.20	41.35
Al_2O_3	36.84	0.96
CaO	0.05	1.08
MgO	0.09	45.65
Na_2O	0.08	< 0.01
K_2O	1.10	< 0.01
Fe_2O_3	0.34	–
FeO	–	6.61
Cr_2O_3	< 0.01	0.19
TiO_2	0.31	< 0.01
NiO	< 0.01	0.27
MnO	< 0.01	0.06
P_2O_5	0.28	< 0.01
$SO_4^{=}$	0.08	< 0.01
Cl^-	0.14	< 0.01
Undetermined	1.19	0.73
LOI	12.30	3.10

Blends were homogenized by attrition milling (milling parameters as well as particle size distribution before and after milling have been already reported and described [1]) and after milling, slurries were dried in an oven at 80 °C in order to obtain powders with about 4 wt% residual H_2O content. Powders were then sieved (300 μm sieve) and uniaxially pressed at 30 MPa into parallelepipedal tiles ($50 \times 70 \times 7$ mm^3). In the present paper, it is worth pointing out that fine powders containing a small quantity of residual water can be easily pressed into parallelepipedal shaped large samples. Pressing parameters were selected in order to replicate industrial conditions.

Green samples were sintered in air, by an industrial electric roller kiln (Nannetti), at 1250 °C in fast firing cycles using a heating rate of 50 °C/min, a cooling rate of 60 °C/min and a dwell time of 10 min (~55 min cold to cold).

Shrinkage on firing was evaluated, by a caliper, along the longest edge (70 mm on green specimens) using the ratio $(\Phi_0-\Phi_1)/\Phi_0$ (subscripts 0 and 1 refer to the sample dimensions before and after the sintering) whereas water absorption was determined following the norm EN99. In line with this procedure, sintered samples were first weighed in air (W_1), then placed into a covered beaker and boiled in water for 2 h. After boiling, samples were cooled in water to room temperature, dried with a cloth and weighed again (W_2). Water absorption was evaluated using the formula: $W(\%) = [(W_2-W_1)/W_1]100$. Apparent density of sintered materials was determined by the, in water, Archimede′s method which implies measurements errors which generally do not exceed 3% of the real value. In the present research we have observed data variation always below 2% which was considered not relevant and therefore not discussed.

In order to evaluate strength and toughness, tiles were cut into bars with dimensions $45 \times 4 \times 6.5$ mm^3. Rupture strength (σ) was evaluated by 4-point bending with a crosshead speed of 0.2 mm min^{-1} using the Shimadzu AG10 equipment; Vickers hardness (H_v) was determined by a 100 N load with a Zwick indenter on polished surfaces (6 μm diamond paste) whereas fracture toughness (K_{IC}) was evaluated by means of Indentation Strength in Bending Method (ISB) breaking specimens indented with a load of 100 N and using the simplified expression $K_{IC} = 0.88\ (\sigma_f P_i^{1/3})^{3/4}\ 1000^{-1/2}$ were σ_f is the precrack strength and P_i the indentation load. All mechanical data reported in the present research have been averaged over 5 measurements.

Crystal phases were investigated by X-ray diffraction (XRD) analysis which was carried out on a Panalytical X′pert Pro Detector X′celerator using monochromated CuKα_1 radiation (40 kV, 40 mA). Spectra were collected using a step size of 0.02° and a counting time of 15 s per angular abscissa in the range 10–80°. The Philips X′Pert HighScore software was used for phase identification with their semi-quantitative evaluation being performed following the RIR method [2].

Microstructures were examined by an Assing EVO40 Scanning Electron Microscope (SEM).

Warpage was determined by the C485-09 ASTM test method. In accordance with it, warpage was calculated as a percentage of the diagonal length of the tiles. It was observed that all tiles examined in the present research showed warpage data below 2.5% and therefore in agreement with earthenware tiles requirements [3].

3. Results

The chemical analysis of K revealed the presence of high quantities of SiO_2, Al_2O_3 and minor fractions of other components in line with literature data [3–5] as is its LOI value; on the other hand, O contains high quantities of SiO_2, MgO, Fe_2O_3, minor quantities of Al_2O_3, CaO and small fractions of NiO, Cr_2O_3 and MnO.

The XRD investigation (Fig. 1) revealed that O powder mainly contains forsterite ($(Mg_{0.672}Fe_{0.323})_2SiO_4$) (JCPDS 01-071-0795), enstatite ($Mg_{1.78}Fe_{0.22}Si_2O_6$) (JCPDS 01-071-1163) and quartz (SiO_2) (JCPDS 01-083-2465) in quantity of

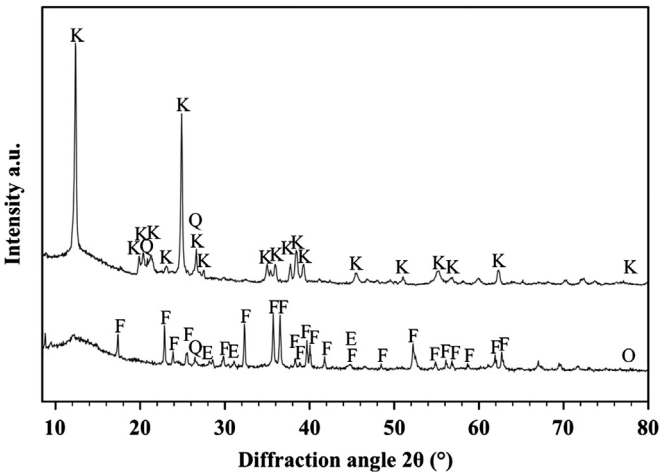

Fig. 1. X-ray diffraction patterns of the as received O and K powders. Identified phases are labelled by the following letters: (E)=enstatite; (F)=forsterite; (Q)=quartz and (K)=kaolinite.

62, 25 and 12 vol% respectively, whereas about 93 vol% kaolinite (JCPDS 01-083-0971) and about 6 vol% of free quartz (JCPDS 01-083-2465) were detected in K; both powders also contain small fractions of other not identified crystal phases.

Fig. 2(a, b) reports the XRD patterns acquired on the free surfaces of the tiles fast fired at 1250 °C. As reported in the introduction item, such temperature was previously identified [1] as optimal sintering temperature, but with different sintering cycle, i.e. with heating and cooling rates of 10 °C min^{-1} and a dwell time of 1 h. Also, using fast firing cycle, the compositions object of the present research turn into materials with low water absorption and limited shrinkage as it can be observed in Table 2. Fig. 2a shows that OK20 contains mullite ($Al_6Si_2O_{13}$) (16%) (JCPDS 01-083-1881), forsterite (33%) and cordierite ($Mg_2Si_5Al_4O_{18}$) (50%) (JCPDS 01-089-1487), same phases as OK40, but with different proportions being mullite (31%), forsterite (29%) and cordierite (39%). Fig. 2b shows that composition OK60 contains forsterite (22%), enstatite (57%) and cordierite (20%) whereas OK80 contains forsterite (19%), enstatite (63%) and spinel ($MgAl_2O_4$) (17%) (JCPDS 01-075-1801). It must be remarked that, in the present research, it was decided to label only phases that were identified by a minimum of 4 representative peaks in line with the Joint Committee of Powder Diffraction Standards. The presence of small amounts of other phases was also revealed, but it was not possible to identify them unambiguously. In all compositions, the presence of vitreous phase is also revealed by the non flat profile of the patterns background line, however those acquired on samples OK20 and OK40 show a greater deviation with respect to those of OK60 and OK80. It seems therefore reasonable to expect that OK20 and OK40 contain a greater amount of glass than materials OK60 and OK80. It is also worth to observe that forsterite is present in the starting powders as well as in all fired samples thus suggesting its great inertness toward the other components of the starting powders.

Table 2 reports water absorption, shrinkage, apparent density, hardness, bending rupture strength and fracture toughness of fired materials. It is possible to observe that water absorption is close to zero in samples with composition OK20, OK40 and OK60 whereas those with composition OK80 display higher value, in line with data previously reported [1]. Also shrinkage of fast fired samples is similar to that observed in materials fired in slow sintering cycle and in both cases the results are in agreement with the official norms for production of many types of tiles [3].

Materials rupture strength was found greater that 50 MPa in all the samples tested as are also their averaged values; it descends that strength data are superior to those required by the official norms for production of most categories of floor tiles which must have a rupture strength greater than 25 MPa [3]. More in detail, Table 2 shows that average strength ranges from 60 MPa for OK20 up to 87 MPa for OK40 somewhat

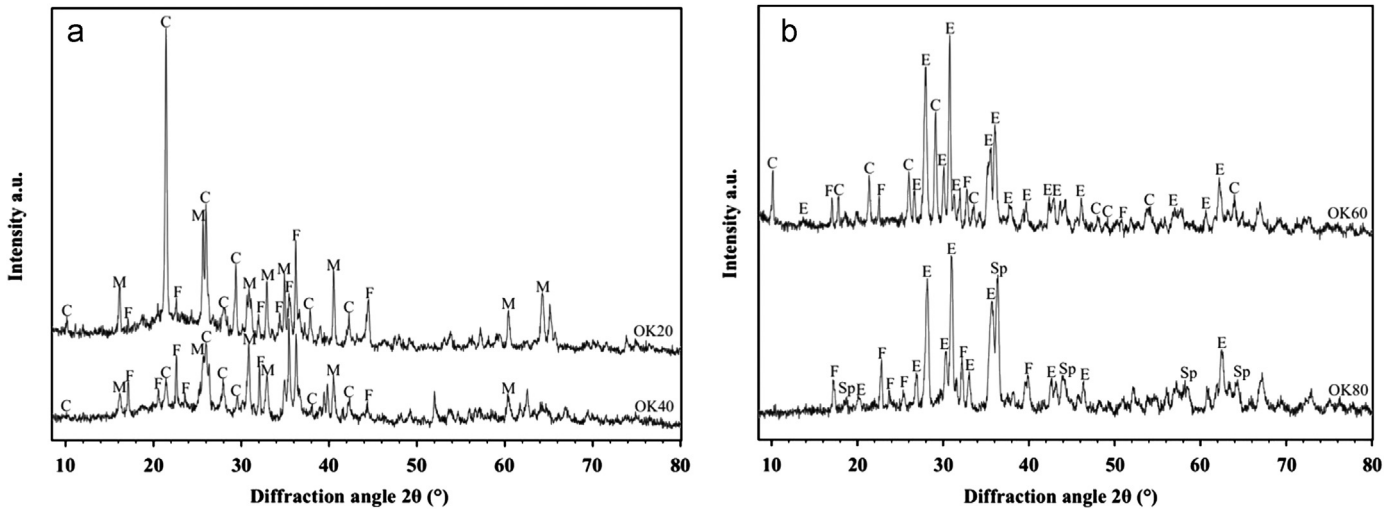

Fig. 2. X-ray diffraction patterns between 10 and 80°, acquired on the free surface of samples OK20 and OK40 (a), and OK60 and OK80 (b). Phases are identified as follows: (C)=cordierite; (M)=mullite; (F)=forsterite; (E)=enstatite and (Sp)=spinel.

Table 2
Water absorption, shrinkage, apparent density (ρ), bending rupture strength (σ), Vickers hardness (H_v) and fracture toughness (K_{Ic}) of the materials fired at 1250 °C with fast cycle.

Material composition	Abs H_2O (%)	Shrinkage (%)	ρ (g/cm^3)	σ (MPa)	H_V (GPa)	K_{IC} (MPa $m^{1/2}$)
OK20	0.2	9.9	2.49	60 ± 5	7.7 ± 0.9	1.7 ± 0.3
OK40	0.1	9.9	2.65	87 ± 3	8.1 ± 0.4	2.2 ± 0.2
OK60	0.8	9.1	2.52	61 ± 6	4.7 ± 1.3	1.6 ± 0.4
OK80	4.2	7.1	3.09	65 ± 5	4.8 ± 1.2	1.1 ± 0.3

higher than those reported for several materials produced using recycled waste [6–11]. Strength data variability is limited, being always limited below 10% of the average value and appears to be independent of material′s composition, but probably affected by their residual closed porosity.

Vickers hardness ranges from a minimum of 4.7 GPa measured on OK60 to a maximum of 8.1 GPa on OK40, suitable for tiles that can be used in both indoor and outdoor areas [3]. However, hardness suffers greater variations with respect to strength, probably due to the presence of a randomly dispersed hidden closed porosity.

Toughness data range from 1.1 $MPam^{1/2}$ measured on OK80 to 2.2 $MPam^{1/2}$ measured on OK20 and are comparable with those of commercial tiles [3].

Table 2 also shows that apparent density ranges from 2.49 g/cm^3 for sample OK20 up to a maximum of 3.09 g/cm^3 for sample OK80. These values are sufficiently in agreement with those usually measured on many floor or wall tiles, table or sanitary ware [3].

SEM photographs, made on free surfaces of the fired samples, are reported in Fig. 3(a–e). Fig. 3a correspond to the microstructure of OK20 and shows a material with a continuous vitreous layer which covers most of the polycrystalline grains. Elongated crystals, with length of 2.5 and thickness of 0.25 μm and therefore with a shape ratio of 10, probably due to secondary mullite [12–15], can be however clearly observed. There is no evident open porosity in agreement with the low water absorption of the samples with this composition (see Table 2).

The surface microstructure of material with composition OK40 (Fig. 3b) is similar to the one of OK20 with no evident open porosity and a continuous vitreous phase which partially covers the polycrystalline grains. However the amount of vitreous phase appears lower and the amount of mullite greater than in composition OK20 in agreement with water absorption data and XRD analysis. Also the shape ratio of mullite crystals appears of same magnitude as for OK20 thus confirming its dependence by thermal cycle more than by the amount of kaolin introduced in this composition [12–14]. The presence of few fractures, probably occurred on cooling after the firing cycle, has also been identified.

Fig. 3c reports the microstructure of composition OK60. The glassy phase is visible also in this material, but its amount appears lower than that observed in OK20 and OK40; conversely open porosity is confirmed higher (see Table 2). The polycrystalline phases which have been identified by the XRD analysis look as equiaxial grains of size smaller than 2 μm; elongated crystals seem to be not present or present in

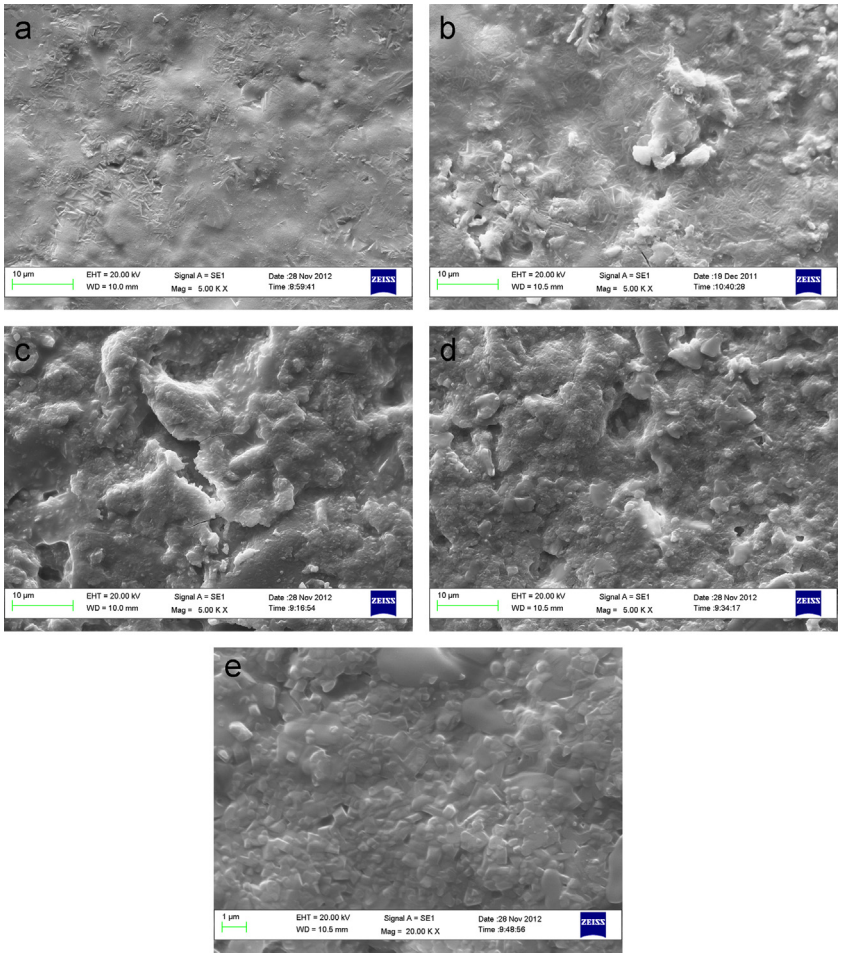

Fig. 3. SEM micrographies (5000 ×) of the as fired surface of samples with composition: (a) OK20, (b) OK40, (c) OK60, and (d) OK80. Fig. 3e shows an enlarged detail of Fig. 3d (20000 ×).

Table 3
Phases, corresponding weight percentage (%), approximate theoretical density (g/cm^3) and relative density (%) of the fired samples.

Sample	Crystalline Phase	Weight (%)	Theoretical density (g/cm^3)	Relative density (%)
	Mullite	16		
OK20	Forsterite	33	2.82	88
	Cordierite	50		
	Mullite	31		
OK40	Forsterite	29	2.85	92
	Cordierite	39		
	Forsterite	22		
OK60	Enstatite	57	3.03	83
	Cordierite	20		
	Forsterite	19		
OK80	Enstatite	63	3.21	96
	Spinel	17		

very small amount. Fig. 3c also documents the presence of large fractures, probably occurred on cooling after the sintering process.

The microstructure of material with composition OK80 shows a reduced amount of vitreous phase, but a higher level of open porosity with respect to the above described compositions. The polycrystalline phases are present as small equiaxial grains with size equal or smaller than 1 μm as it can be confirmed by Fig. 3e which is a high magnification image of the same microstructure; elongated crystals are not visible and the presence of large fractures is not documented.

Based on the above described XRD analysis and using theoretical density data reported by the PDF of each phase, it is possible to calculate, using the rules of mixtures, indicative values of the theoretical density of each material after the firing process. In this procedure, in addition to the identified crystal phases, it is also necessary to include, in each material, an approximate amount of glass, arbitrary assumed as 15 vol% for OK20 and OK40 and as 5 vol% for OK60 and OK80 respectively as a result of the SEM investigation.

The used literature theoretical density values for the crystalline phases are as follows: cordierite 2.65 g/cm^3, enstatite and forsterite 3.2, spinel 3.7 and mullite 3.1. The density of the glass phase was set 2.50 g/cm^3, same for all compositions, as this is the value which literature reports for most of the Na/Ca glass for windows and seem to be reasonably similar to the glass present in our samples which contain great amounts of SiO_2, MgO and Al_2O_3. As result of the above procedure, the following theoretical densities have been determined: 2.82 g/cm^3 for OK20, 2.85 for OK40, 3.03 for OK60 and 3.21 for OK80.

Such values can be compared to the apparent density data reported in Table 2. By the ratio between apparent density and theoretical density it is possible to calculate the relative density of each material which is 88% for OK20, 92.7 for OK40, 83% for OK60 and 96% for OK80. Such results together with crystallographic characteristics are summarized in Table 3. If such values are associated to the mechanical properties reported in Table 2 it can be observed that materials behaviour follows relative density, except composition OK80 which displays the highest relative density but, at the same time, the highest total porosity. In definitive it can be stated that materials properties are greatly affected by their closed porosity, being the maximum strength limited by the strength of the glassy phase. It seems also that the crystallographic structures have a second level influence on materials mechanical properties.

It can be concluded that all the compositions described in the present paper display limited water absorption and shrinkage, sufficiently good strength, hardness and toughness and therefore their behaviour is in line with the requirements for the industrial production of some commercial tiles, but the behaviour of composition OK40 is close to that of porcelanized stoneware [3]. Also in consideration that warpage of all the tiles produced is low and then in line the official norms for production, work is now in progress in order to point out the industrial production of olivine–kaolin glazed tiles.

4. Concluding remarks

In the present work were prepared and characterized several ceramics containing olivine powder and a natural kaolin. Powders blends, mixed by wet attrition milling, dried, sieved and pressed into tiles were fast fired, 55 min cold to cold, at 1250 °C. Tiles samples were characterized by water absorption, shrinkage, apparent density, XRD, flexural rupture strength, hardness, toughness, microstructure and warpage. It is demonstrated that materials behaviour depends on amount of vitreous phase and on amount of their total porosity including open and close porosity. It is also observed that all compositions could be suitable for an eventual industrial production of some commercial tiles, but those with composition containing 60% olivine and 40% kaolin displayed the best overall behaviour.

References

[1] E. Furlani, G. Tonello, E. Aneggi, S. Maschio, Possible use of waste olivine powders from a foundry process into the ceramic industry: sintering behaviour of olivine, kaolin and their blends, Ceramics International 39 (2013) 1257–1263.
[2] R. Jenkins, R. Snyder, Introduction to X-ray powder diffractometry, Wiley, New York, 1996.

[3] T. Manfredini, G.C. Pellacani, Engineering Materials Handbook, Ceramics and Glasses—ASTM 4 (1992) 925–929.
[4] W.D. Kingery, Introduction to Ceramics, John Wiley and Sons Inc New York, 1976.
[5] M.N. Rahaman, Ceramic, Processing and Sintering, 2nd ed., Marcel Dekker, New York, 2003.
[6] C. Fiori, A. Brusa, Iron slags containing body for the production of wall tiles by a rapid single firing techniques, Ceramic Powder, Elsevier New York161–172.
[7] D. Baruzzo, D. Minichelli, S. Bruckner, L. Fedrizzi, A. Bachiorrini, S. Maschio, Possible production of ceramic tiles from marine dredging spoils alone and mixed with other waste materials, Journal of Hazardous Materials 134 (2006) 202–210.
[8] A. Olgun, Y. Erdogan, Y. Ayhan, B. Zeybek, Development of ceramic tiles from coal fly ash and tincal ore waste, Ceramics International 31 (2005) 153–158.
[9] V.K. Marghussian, A. Magsoodipoor, Fabrication of unglazed floor tiles containing Iranian copper slag, Ceramics International 25 (1999) 617–622.
[10] L. Barbieri, I. Lancellotti, T. Manfredini, I. Queralt, J.Ma Rincon, M. Romero, Design, obtainment and properties of glasses and glass–ceramics from coal fly ash, Fuel 78 (1999) 271–276.
[11] M. Romero, J.Ma Rincón, R.D. Rawlings, A.R. Boccaccini, Use of vitrified urban incinerator waste as raw material for production of sintered glass–ceramics, Materials Research Bulletin 36 (2001) 383–395.
[12] J. Martin-Marquez, J.Ma Rincon, M. Romero, Mullite development on firing in porcelain stoneware bodies, Journal of the European Ceramic Society 30 (2010) 1599–1607.
[13] W.E. Lee, Y. Iqbal, Influence of mixing on mullite formation in porcelain, Journal of the European Ceramic Society 21 (2001) 2583–2586.
[14] W.E. Lee, G.P. Souza, C.J. McConville, T. Tarvornpanich, Y. Iqbal, Mullite formation in clays and clay-derived vitreous ceramics, Journal of the European Ceramic Society 28 (2008) 465–471.
[15] J.M. Perez, J.Ma Rincon, M. Romero, Effect of moulding pressure on microstructure and technological properties of porcelain stoneware, Ceramics International 38 (2012) 317–325.